Supporting Information

A single probe to sense Al(III) colorimetrically and Cd(II) by turn-on fluorescence in physiological conditions and live cells, corroborated by X-ray crystallographic and theoretical studies

Chirantan Kar[a], Soham Samanta[a], Sudeep Goswami[b], Aiyagari Ramesh[b] and Gopal Das*[a]*

[a] Department of Chemistry, Indian Institute of Technology Guwahati, Assam, 781 039, India.

[b] Department of Biotechnology, Indian Institute of Technology Guwahati, Assam, 781 039, India.

E-mail: gdas@iitg.ernet.in; aramesh@iitg.ernet.in

Fax: +91-361-258-2349; Tel: +91-361-258-2313

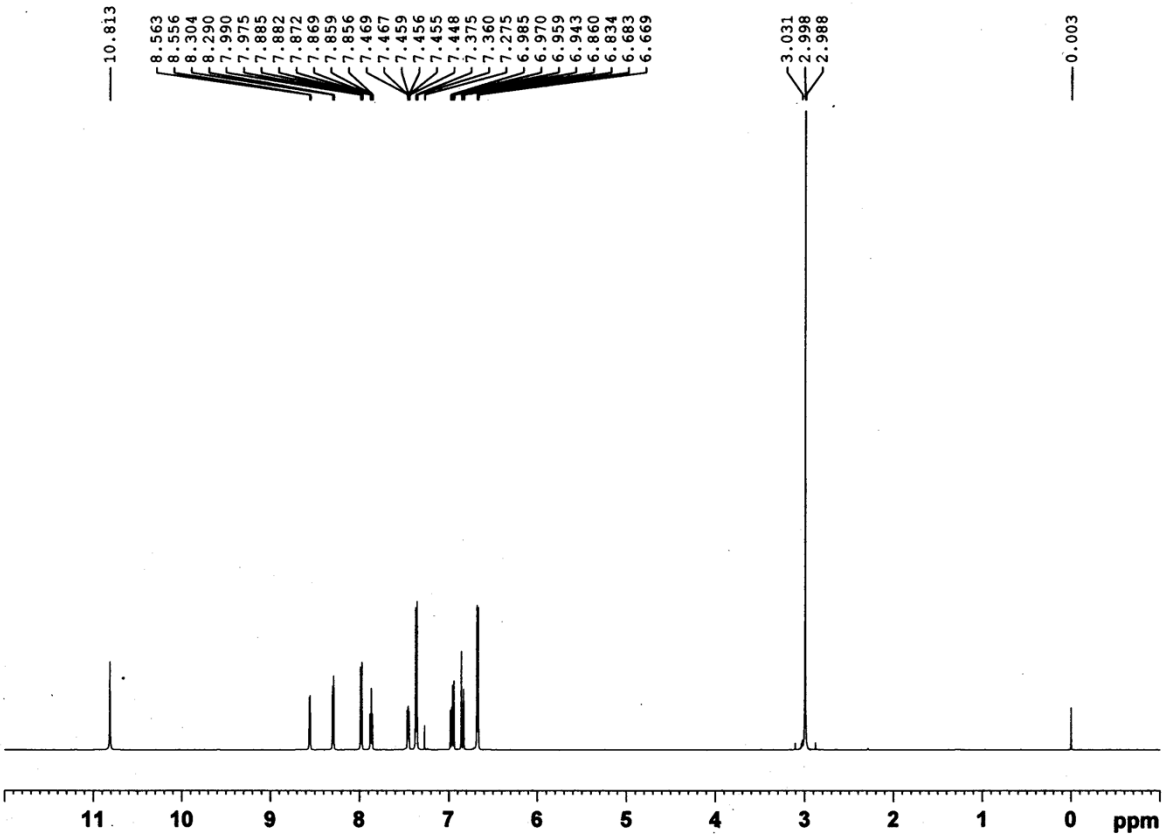

Figure S1: ^{1}H NMR spectrum of $\mathbf{L_1}$ in $CDCl_3$ solution.

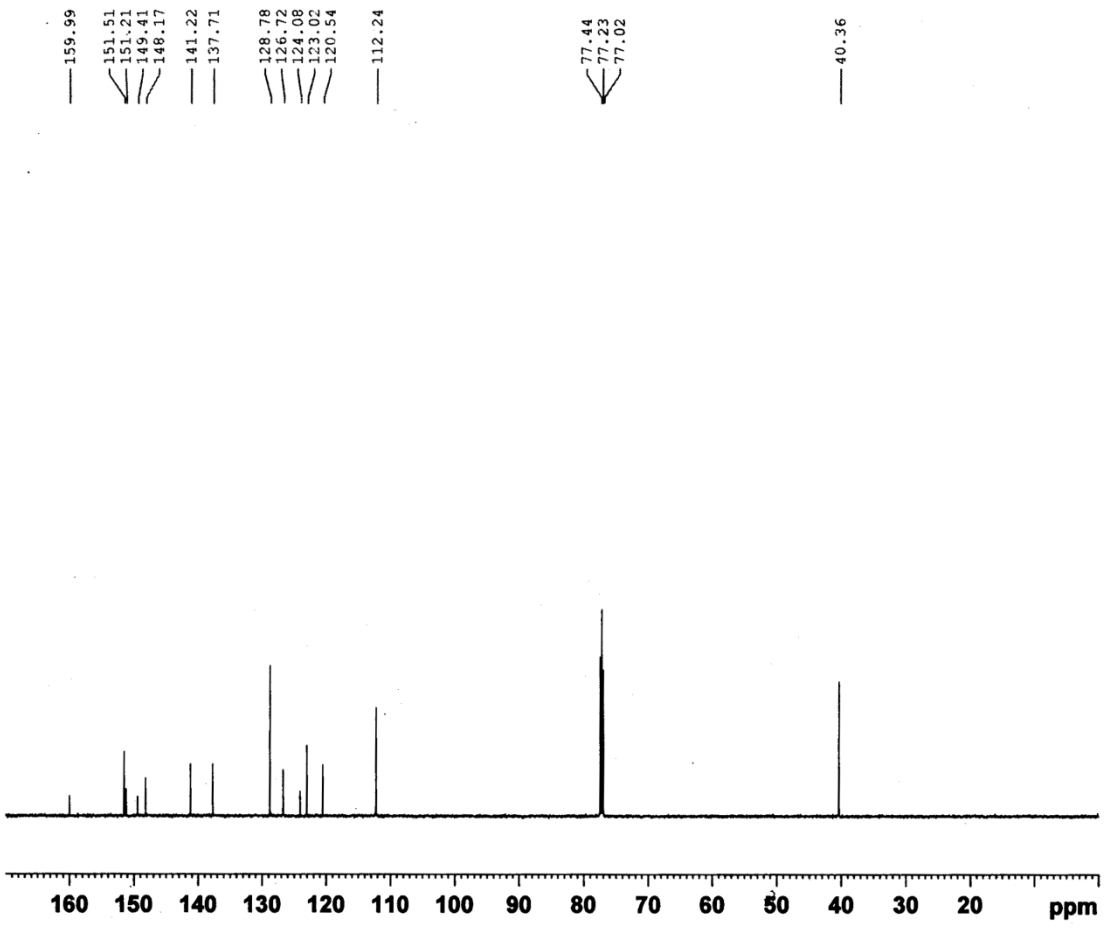

Figure S2: ^{13}C NMR spectrum of $\mathbf{L_1}$ in $CDCl_3$ solution.

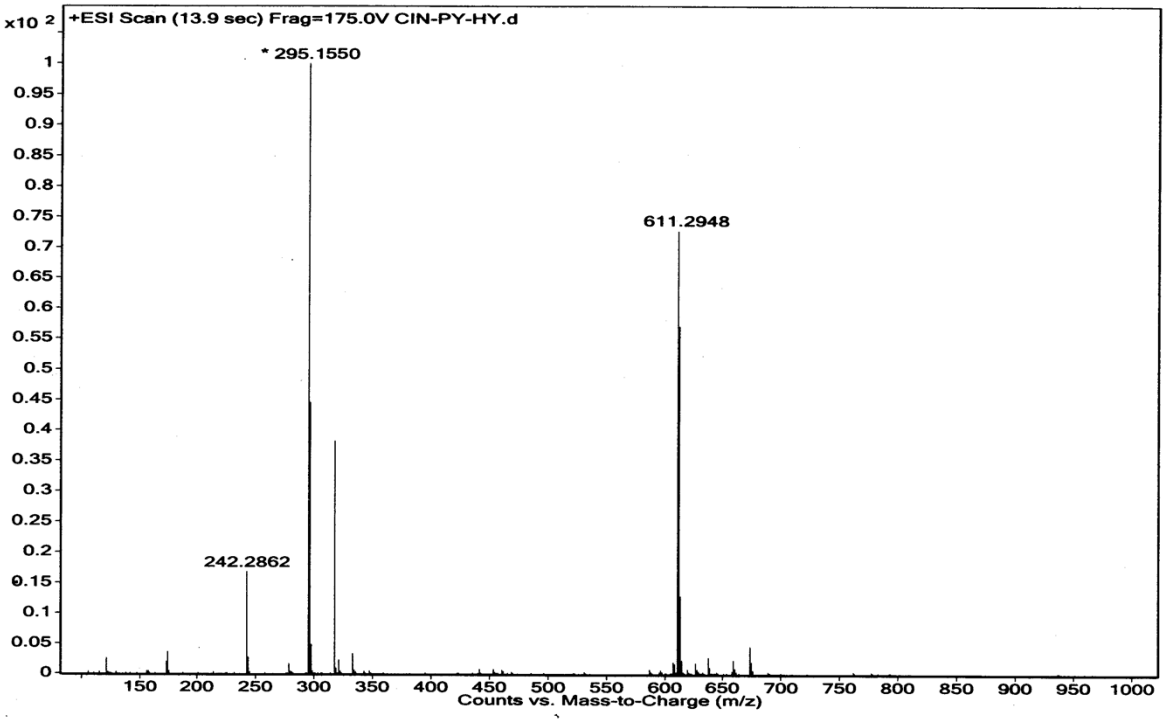

Figure S3: Mass spectrum of $\mathbf{L_1}$ (Mass spectrum obtained in positive mode)**.**

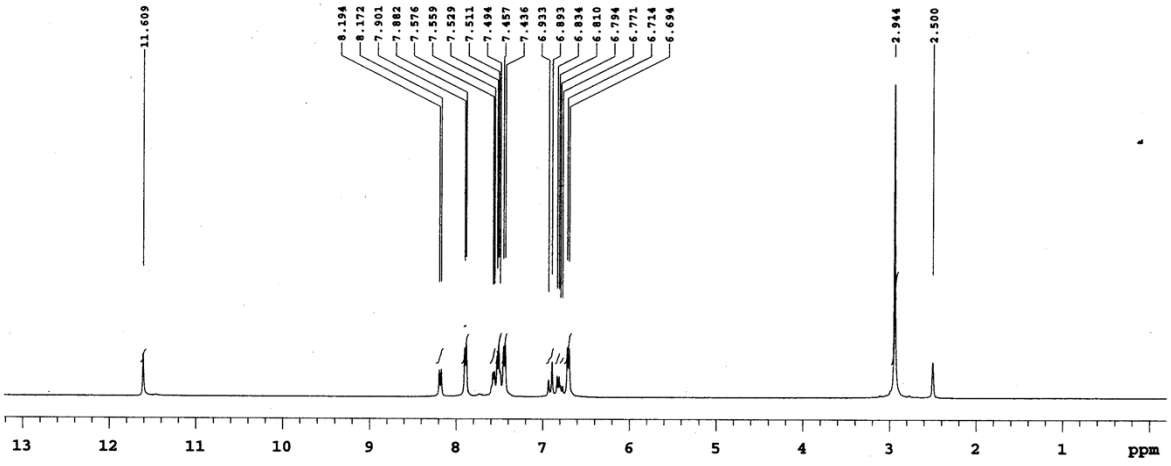

Figure S4: ^{1}H NMR spectrum of $\mathbf{L_2}$ in $CDCl_3$ solution.

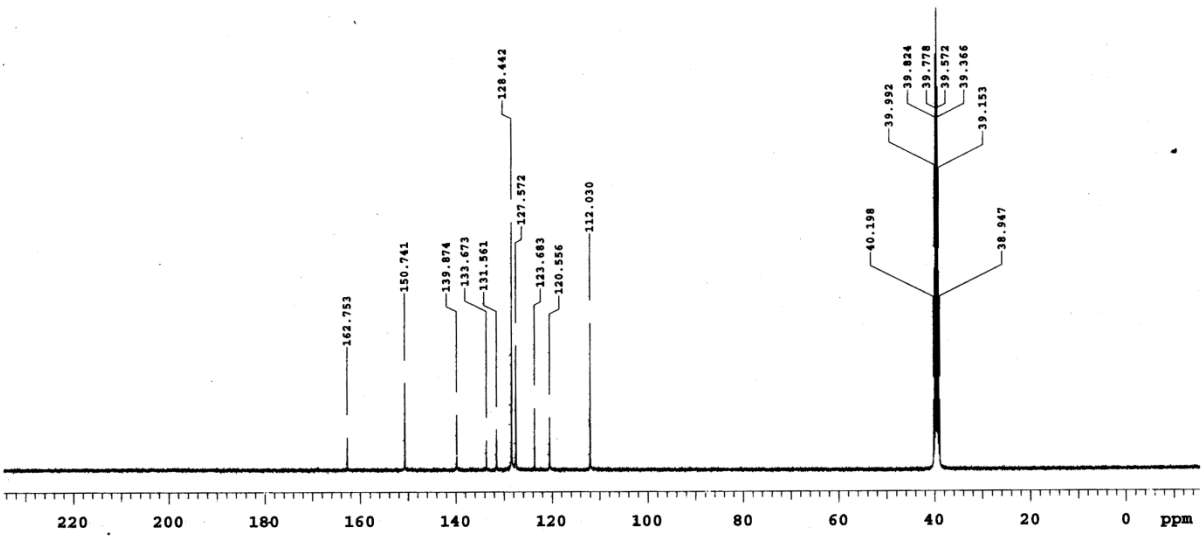

Figure S5: ^{13}C NMR spectrum of $\mathbf{L_2}$ in $CDCl_3$ solution.

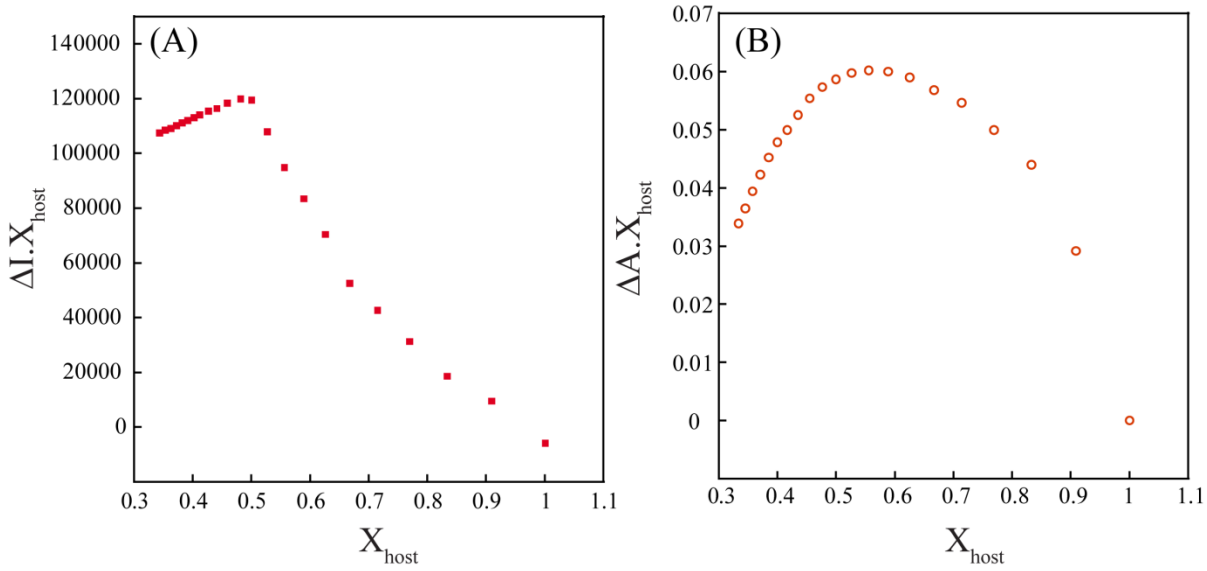

Figure S6: (A) Job's plot between $\mathbf{L_1}$ and Cd^{2+} ions. Where X_{host} = the mole fraction of $\mathbf{L_1}$ and ΔI is the change $(I-I_0)$ in the intensity of the emission spectra in presence of guest. (B) Job's plot between $\mathbf{L_1}$ and Al^{3+} ions. Where X_{host} = the mole fraction of $\mathbf{L_1}$ and ΔA is the change $(A-A_0)$ in the absorbance at 510 nm of the UV-Vis spectra in presence of guest.

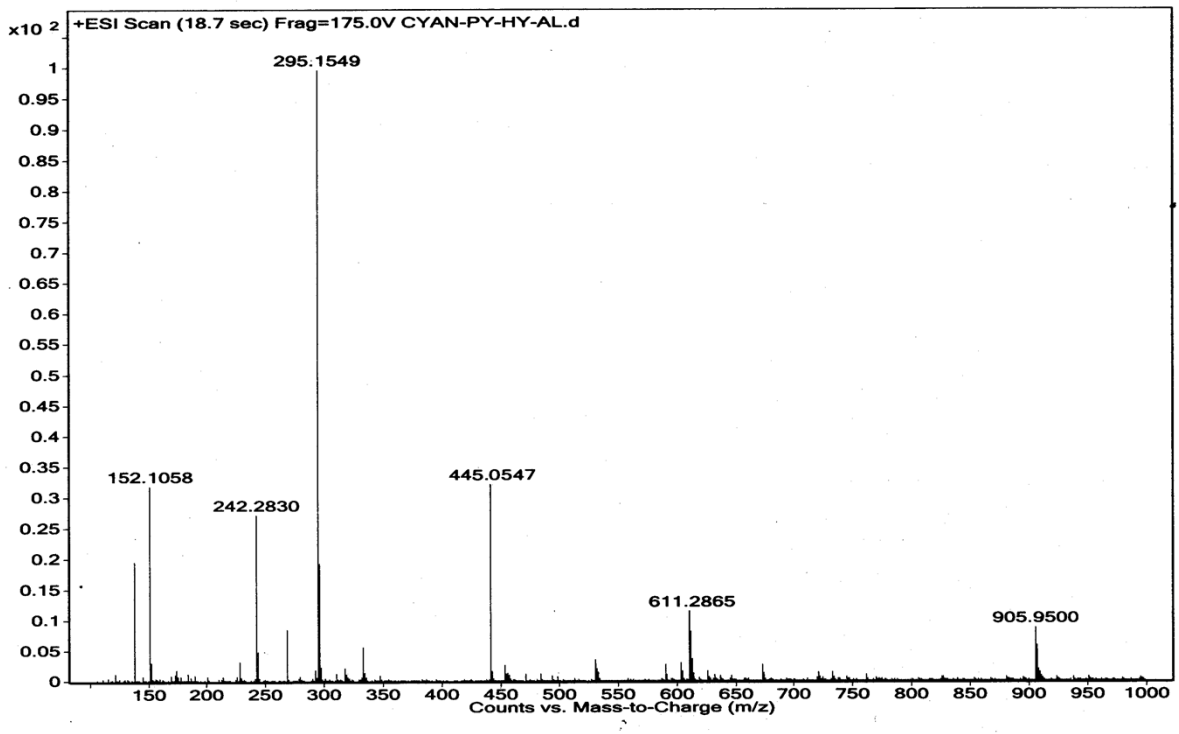

Figure S7: Mass spectrum of **L_1-Al** complex.

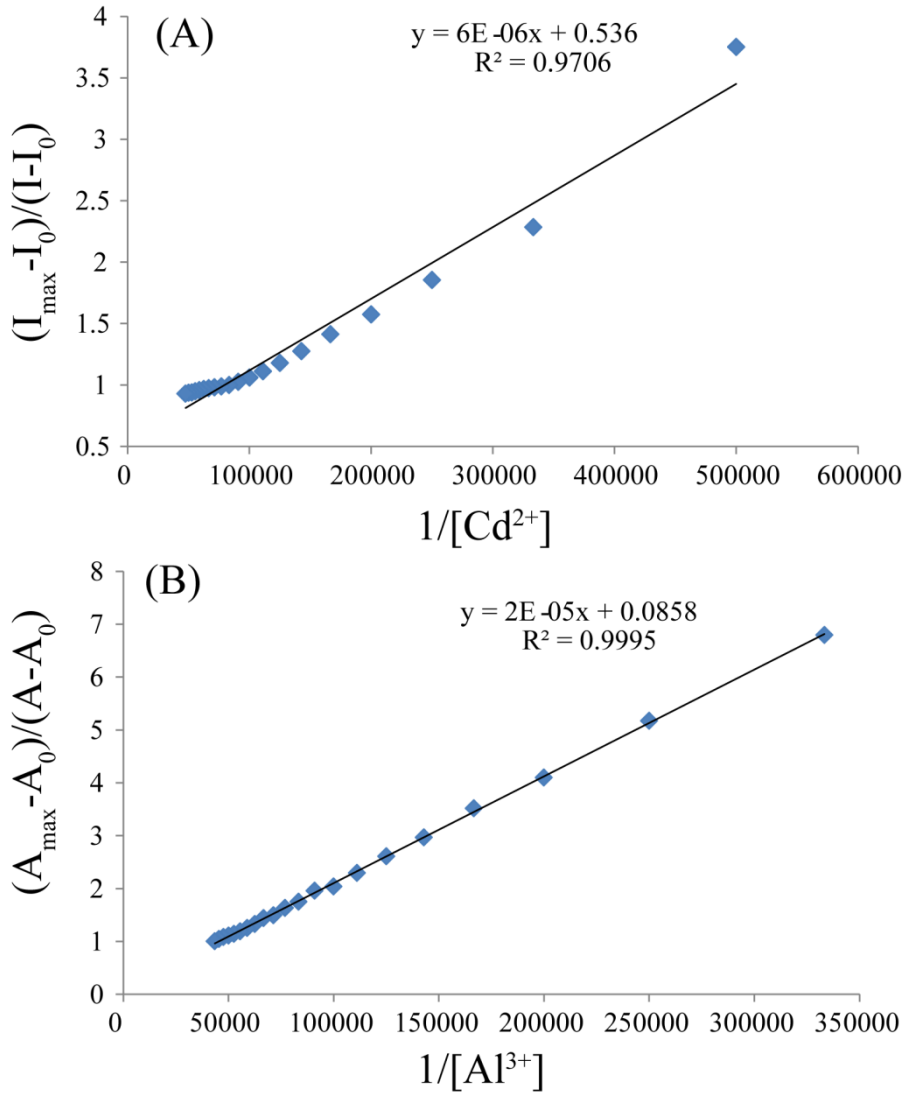

Figure S8: (A) Bensei-Hildebrand plot for **L_1-Cd** complex obtained from the fluorescence emission (calculated at λ_{em}) studies. (B) Bensei-Hildebrand plot for **L_1-Al** complex obtained from the UV-Vis studies (calculated at λ= 510nm) studies.

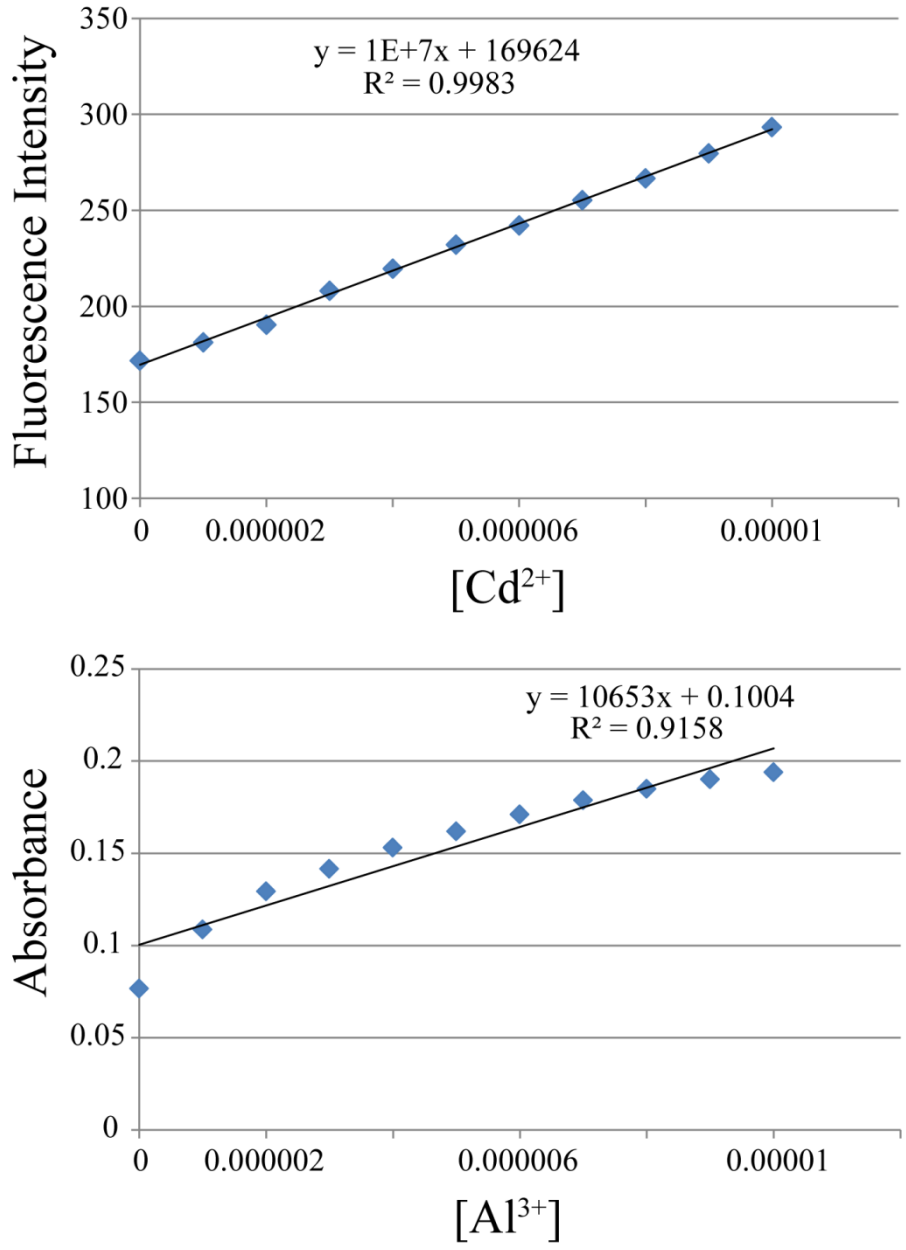

Figure S9: (A) Intensity versus Concentration plot for measuring the detection limit (3σ/k, here σ=11.657) of Cd^{2+} by **L**[1]. (B) Intensity versus Concentration plot for measuring the detection limit (3σ/k, here σ=0.030888) of Al^{3+} by **L**[1].

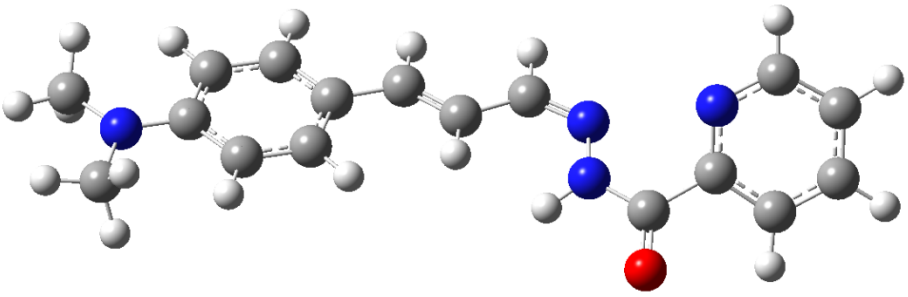

Figure S10: Optimized structure of $\mathbf{L_1}$ at B3LYP/6-31+ G(d,p).

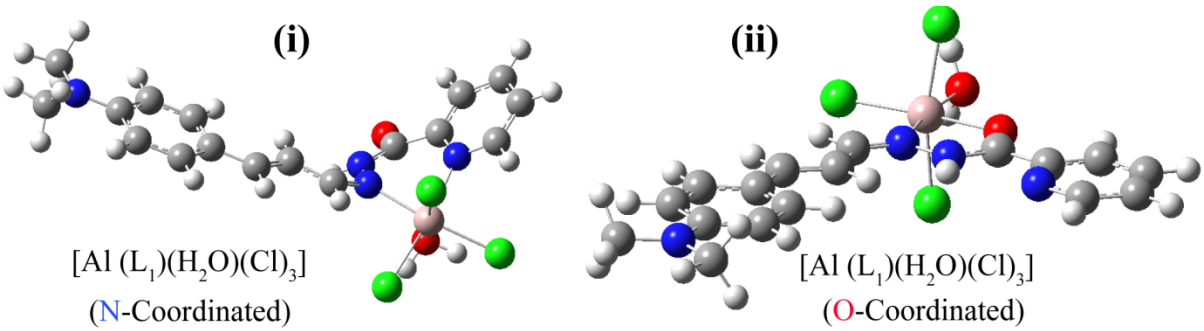

Figure S11. Optimized proposed structures of $\mathbf{L_1}$-Al^{3+} complex at B3LYP/6-31+ G(d,p) (**i**) coordination through pyridine-N (b) coordination through carbonyl-O.

Table S1. Calculated total energies of $\mathbf{L_1}$ and $\mathbf{L_1}$-Al^{3+} complex at B3LYP/6-31+ G(d,p)

Molecule	Total Energy (a.u.)
L_1	-952.85647086
L_1-Al^{3+} Complex (N-Coordinated) [Structure (**i**)]	-2652.59357349
L_1-Al^{3+} Complex (O-Coordinated) [Structure (**ii**)]	-2652.60637327

Structure **(ii)** is more stable by 8.01 kcal/mole than the structure **(i)**

Coordinates for optimized geometry of $\mathbf{L_1}$ at B3LYP/6-31+ G(d,p).

Center Number	Atomic Number	Atomic Type	Coordinates (Angstroms) X	Y	Z

1	6	0	3.723277	-1.657780	-0.420719
2	6	0	2.634455	-0.788824	-0.217420
3	6	0	2.946128	0.534725	0.155113
4	6	0	4.252358	0.961667	0.318962
5	6	0	5.344118	0.077511	0.122704
6	6	0	5.038689	-1.249353	-0.262741
7	1	0	3.527721	-2.686120	-0.715114
8	1	0	2.147965	1.252222	0.320253
9	1	0	4.429590	1.991895	0.601117
10	1	0	5.831694	-1.964763	-0.439962
11	6	0	1.279979	-1.283328	-0.400327
12	6	0	0.112177	-0.609468	-0.259545
13	1	0	1.212517	-2.333740	-0.686904
14	1	0	0.129867	0.435694	0.038527
15	6	0	-1.166637	-1.261673	-0.450616
16	1	0	-1.145483	-2.337525	-0.623211
17	6	0	-4.951184	0.467229	0.031990
18	6	0	-6.132266	0.890060	-0.589185
19	6	0	-7.315742	0.222221	-0.288393
20	1	0	-6.100715	1.725077	-1.279338
21	6	0	-6.052613	-1.141963	1.224620
22	6	0	-7.278183	-0.818878	0.638056
23	1	0	-8.249246	0.512389	-0.761517
24	1	0	-5.991562	-1.935430	1.967308
25	1	0	-8.175799	-1.365736	0.909196
26	7	0	6.647714	0.494555	0.304648

27	7	0	-4.904142	-0.525092	0.931702
28	6	0	-3.696815	1.244029	-0.268550
29	8	0	-3.735339	2.454310	-0.469549
30	7	0	-2.486917	0.587926	-0.284731
31	1	0	-1.704094	1.212181	-0.465158
32	7	0	-2.360898	-0.764307	-0.440212
33	6	0	6.931766	1.889364	0.598148
34	1	0	8.006038	2.014215	0.737087
35	1	0	6.611828	2.563436	-0.209781
36	1	0	6.437781	2.211094	1.522882
37	6	0	7.746312	-0.402532	-0.011004
38	1	0	8.690432	0.092268	0.218714
39	1	0	7.697437	-1.320154	0.588060
40	1	0	7.761540	-0.691091	-1.072167

Rotational constants (GHZ): 1.0804546 0.0699011 0.0670133

Coordinates for optimized geometry of **L_1-**Al^{3+} complex at B3LYP/6-31+ G(d,p),

Structure **i**

Center Number	Atomic Number	Atomic Type	Coordinates (Angstroms) X	Y	Z
1	6	0	-4.780313	-1.413635	0.620151
2	6	0	-3.811086	-0.483185	0.186705
3	6	0	-4.287227	0.765794	-0.272506
4	6	0	-5.633946	1.066849	-0.297560
5	6	0	-6.605432	0.124319	0.139820

6	6	0	-6.133196	-1.131358	0.601734
7	1	0	-4.452267	-2.385332	0.980087
8	1	0	-3.584695	1.518903	-0.615809
9	1	0	-5.943649	2.039659	-0.657312
10	1	0	-6.829234	-1.885159	0.946092
11	6	0	-2.417495	-0.844641	0.233085
12	6	0	-1.335025	-0.103639	-0.147051
13	1	0	-2.213444	-1.843211	0.619467
14	1	0	-1.454930	0.902126	-0.536480
15	6	0	-0.022437	-0.641236	0.007953
16	1	0	0.092025	-1.603802	0.497466
17	6	0	3.075936	2.027147	-0.084008
18	6	0	3.584921	3.278196	0.269193
19	6	0	4.539321	3.361929	1.277392
20	1	0	3.215266	4.148928	-0.257406
21	6	0	4.432866	0.974700	1.468391
22	6	0	4.959223	2.188403	1.897696
23	1	0	4.943189	4.324771	1.574493
24	1	0	4.748500	0.034382	1.901261
25	1	0	5.692490	2.197897	2.696085
26	7	0	-7.944901	0.419838	0.115405
27	6	0	2.002475	2.028954	-1.142625
28	8	0	1.919186	2.947945	-1.947837
29	7	0	1.037019	1.059076	-1.107265
30	1	0	0.370756	1.103046	-1.871617
31	7	0	1.111918	-0.123477	-0.378735
32	6	0	-8.403513	1.716907	-0.361368

33	1	0	-9.491536	1.751402	-0.312629
34	1	0	-8.011113	2.538624	0.251411
35	1	0	-8.106566	1.894397	-1.402665
36	6	0	-8.918904	-0.558481	0.578276
37	1	0	-9.920227	-0.139376	0.483087
38	1	0	-8.880430	-1.481153	-0.014561
39	1	0	-8.760586	-0.821954	1.631801
40	7	0	3.511756	0.885250	0.490104
41	17	0	5.160098	-1.675435	-0.192112
42	17	0	2.448881	-1.691459	1.974907
43	17	0	2.113370	-2.896918	-1.284841
44	8	0	3.361292	-0.368296	-2.053841
45	1	0	2.961807	-1.111043	-2.549127
46	1	0	4.319617	-0.563987	-2.046965
47	13	0	2.945671	-1.122958	-0.112054

Rotational constants (GHZ): 0.2758046 0.0556066 0.0510078

Structure **ii**

Center Number	Atomic Number	Atomic Type	Coordinates (Angstroms) X	Y	Z

1	6	0	-4.771213	-1.653961	-0.000178
2	6	0	-3.712671	-0.720827	-0.000160
3	6	0	-4.069594	0.645907	-0.000074
4	6	0	-5.388653	1.054419	-0.000014
5	6	0	-6.450324	0.108787	-0.000040
6	6	0	-6.098164	-1.265002	-0.000114

7	1	0	-4.536393	-2.715177	-0.000236
8	1	0	-3.295922	1.407670	-0.000054
9	1	0	-5.605330	2.115010	0.000056
10	1	0	-6.866512	-2.027389	-0.000116
11	6	0	-2.352049	-1.200100	-0.000217
12	6	0	-1.195757	-0.477300	-0.000153
13	1	0	-2.246245	-2.284794	-0.000315
14	1	0	-1.233826	0.608426	-0.000034
15	6	0	0.062593	-1.155452	-0.000201
16	1	0	0.076181	-2.242855	-0.000287
17	6	0	2.934039	2.602926	0.000153
18	6	0	4.227788	3.125094	0.000335
19	6	0	4.368224	4.511613	0.000361
20	1	0	5.076190	2.451227	0.000448
21	6	0	1.971226	4.679328	0.000026
22	6	0	3.221970	5.304401	0.000204
23	1	0	5.354857	4.963922	0.000501
24	1	0	1.057957	5.269572	-0.000101
25	1	0	3.287531	6.387301	0.000217
26	7	0	-7.763048	0.511356	0.000000
27	7	0	1.819460	3.353689	0.000000
28	6	0	2.727983	1.132328	0.000111
29	8	0	3.671672	0.318194	0.000216
30	7	0	1.450417	0.707413	-0.000048
31	1	0	0.701578	1.390773	-0.000200
32	6	0	-8.098089	1.927682	0.000234
33	1	0	-9.182163	2.038567	0.000195

34	1	0	-7.706354	2.438743	0.889127
35	1	0	-7.706276	2.439025	-0.888458
36	6	0	-8.830513	-0.478041	0.000118
37	1	0	-9.792856	0.033162	0.000063
38	1	0	-8.788918	-1.120940	-0.888455
39	1	0	-8.788916	-1.120777	0.888815
40	7	0	1.261316	-0.650480	-0.000146
41	17	0	3.327584	-1.492274	2.266072
42	17	0	3.328180	-1.491854	-2.266047
43	17	0	2.238202	-3.712901	-0.000340
44	8	0	5.025555	-2.260014	0.000193
45	1	0	5.147516	-2.806892	-0.793398
46	1	0	5.147293	-2.806882	0.793826
47	13	0	3.112891	-1.641408	-0.000040

Rotational constants (GHZ): 0.1862056 0.0603920 0.0488042

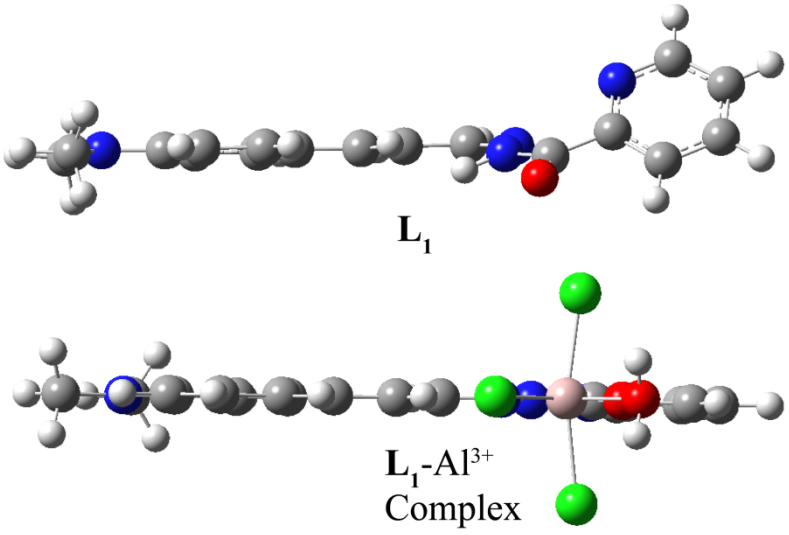

Figure S12: Comparison of the planarity between $\mathbf{L_1}$ and its Al-complex (structure **i**)

Table S2. Selected orbitals and their energies for $\mathbf{L_1}$ at B3LYP/6-31+ G(d,p).

Occupied Orbitals	Energy (eV)	Vacant Orbitals	Energy (eV)
HOMO -2 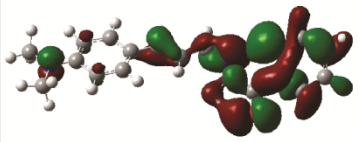	-6.4341	LUMO 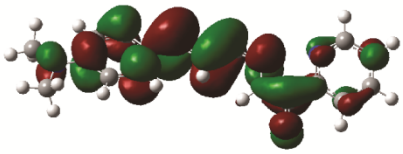	-1.4798
HOMO -1 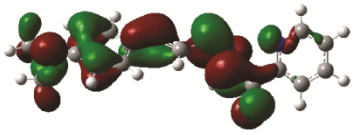	-6.0915	LUMO+1 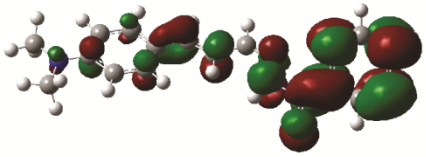	-0.8923
HOMO 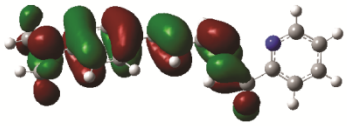	-5.0080	LUMO+2 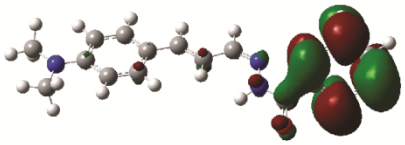	-0.3510

Table S3. Selected orbitals and their energies for **L_1**-Al complex (structure **ii**) at B3LYP/6-31+ G(d,p).

Occupied Orbitals	Energy (eV)	Vacant Orbitals	Energy (eV)
HOMO -2 	-6.2757	LUMO 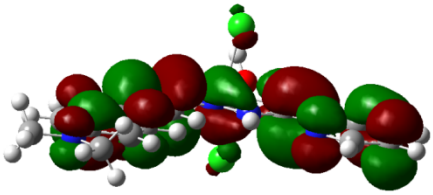	-2.5527
HOMO -1 	-5.8417	LUMO+1 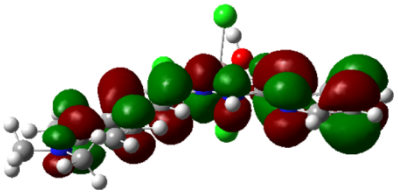	-1.9257
HOMO 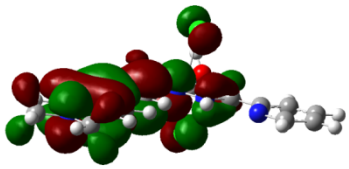	-5.6332	LUMO+2 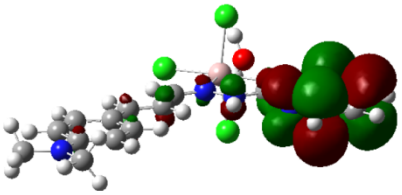	-1.3108

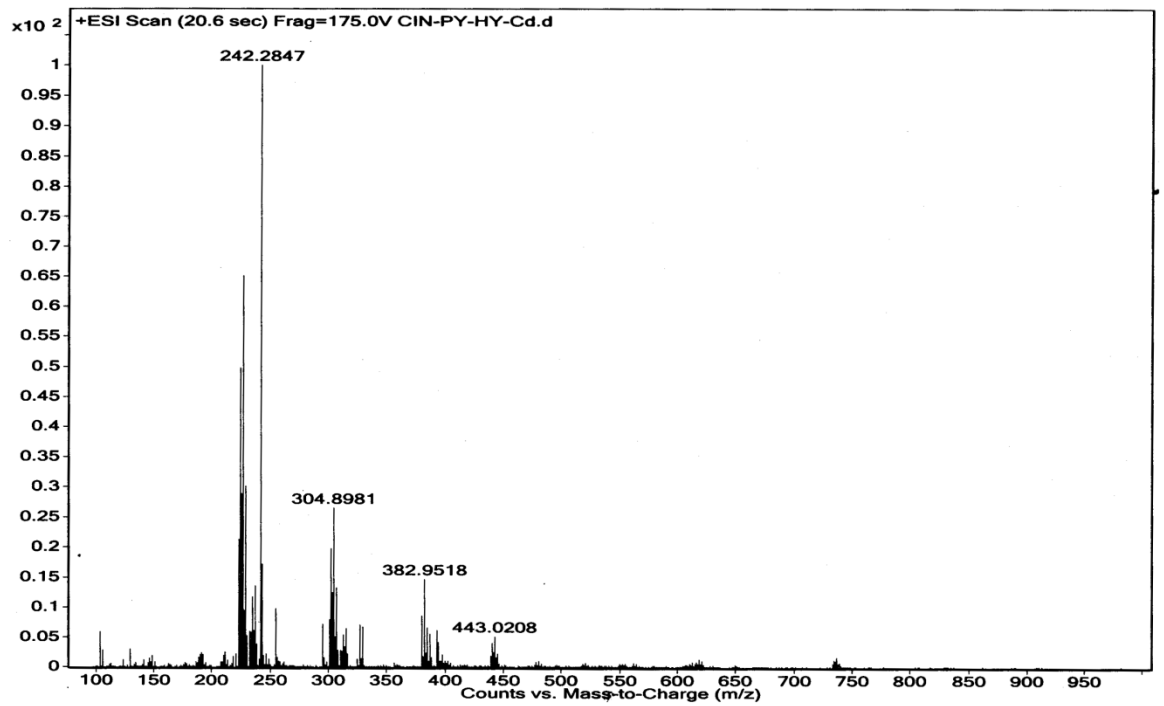

Figure S13: Mass spectrum of the solution containg $\mathbf{L_1}$ in presence of Cd^{2+} ions.

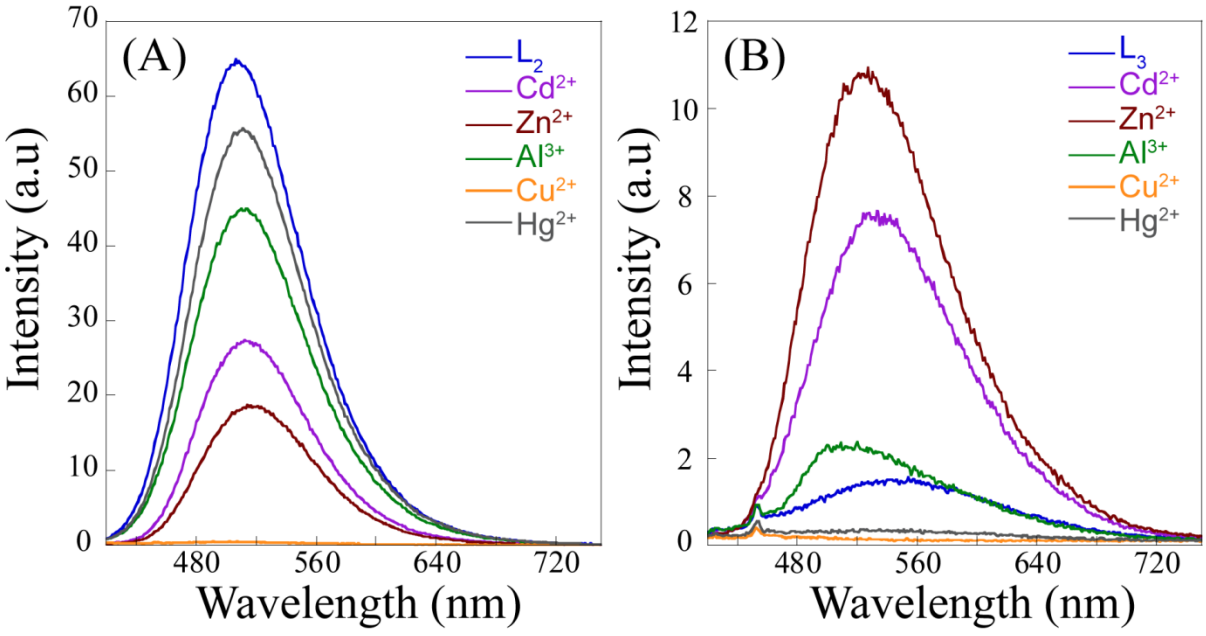

Figure S14: Fluorescence spectra of $\mathbf{L_2}$ and $\mathbf{L_3}$ in presence of various cations.

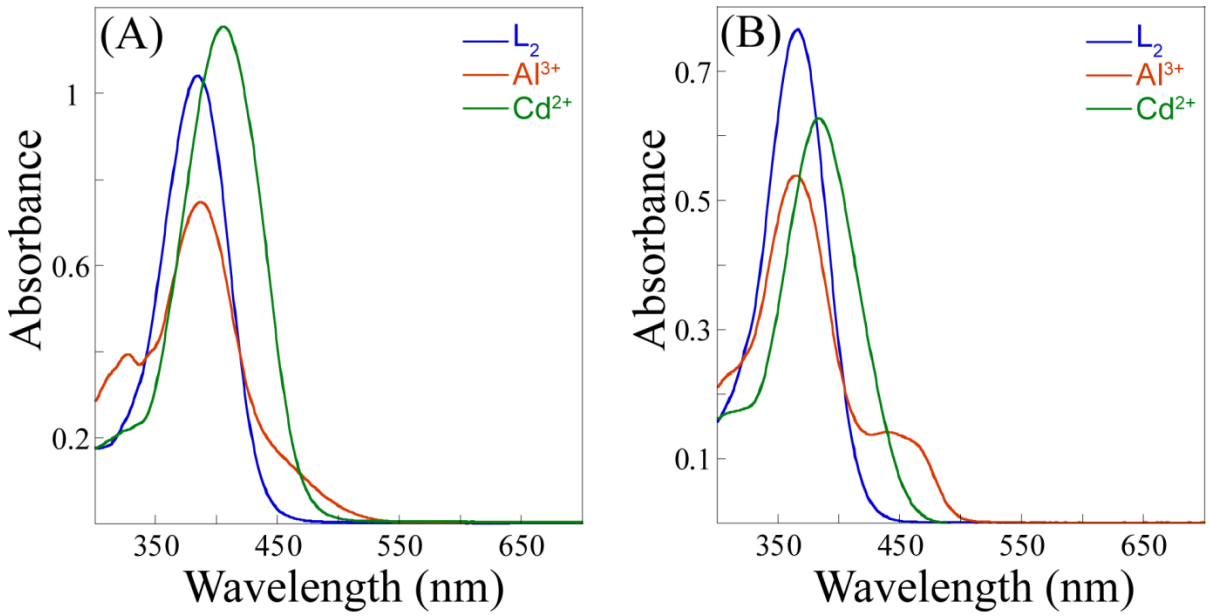

Figure S15: UV-Vis spectra of $\mathbf{L_2}$ and $\mathbf{L_3}$ in presence of Al^{3+} and Cd^{2+}.

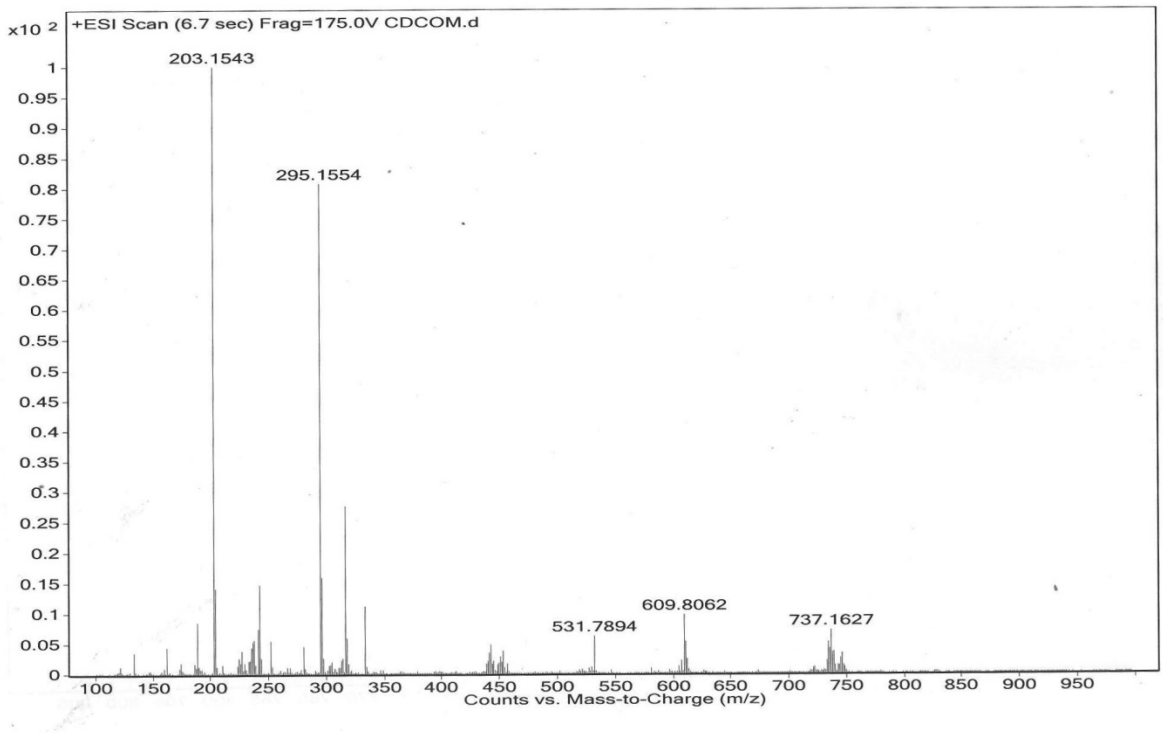

Figure S16: Mass spectrum of the $\mathbf{L_1}$**-Cd** crystal

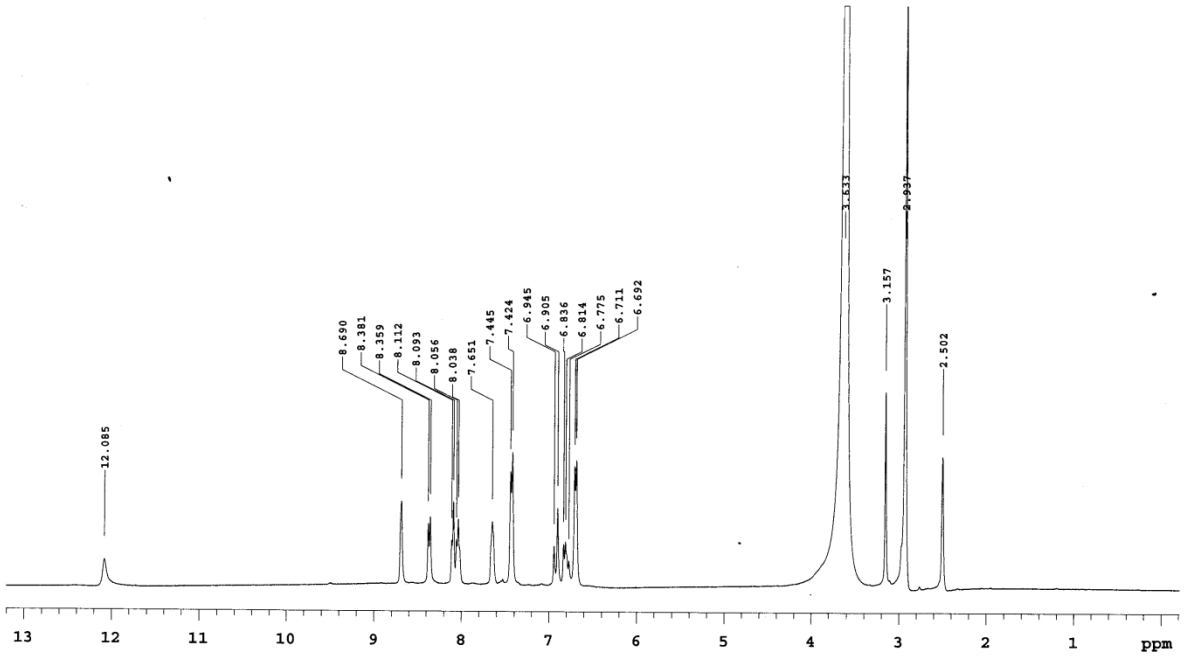

Figure S17: ^{1}H NMR spectrum of the **L_1-Cd** crystals in d_6 DMSO solution.

References:

1. Koch, W.; Holthausen, M. C. *A Chemist's Guide to Density Functional Theory. 2nd edition,* Wiley-VCH, New York, **2000**, 1-300.

2. Gaussian 03, Revision E.01, M. J. Frisch, G. W. Trucks, H. B. Schlegel, G. E. Scuseria, M. A. Robb, J. R. Cheeseman, J. A. Montgomery, Jr., T. Vreven, K. N. Kudin, J. C. Burant, J. M. Millam, S. S. Iyengar, J. Tomasi, V. Barone, B. Mennucci, M. Cossi, G. Scalmani, N. Rega, G. A. Petersson, H. Nakatsuji, M. Hada, M. Ehara, K. Toyota, R. Fukuda, J. Hasegawa, M. Ishida, T. Nakajima, Y. Honda, O. Kitao, H. Nakai, M. Klene, X. Li, J. E. Knox, H. P. Hratchian, J. B. Cross, V. Bakken, C. Adamo, J. Jaramillo, R. Gomperts, R. E. Stratmann, O. Yazyev, A. J. Austin, R. Cammi, C. Pomelli, J. W. Ochterski, P. Y. Ayala, K. Morokuma, G. A. Voth, P. Salvador, J. J. Dannenberg, V. G. Zakrzewski, S. Dapprich, A. D. Daniels, M. C. Strain, O. Farkas, D. K. Malick, A. D. Rabuck, K. Raghavachari, J. B. Foresman, J. V. Ortiz, Q. Cui, A. G. Baboul, S. Clifford, J. Cioslowski, B. B. Stefanov, G. Liu, A. Liashenko, P. Piskorz, I. Komaromi, R. L. Martin, D. J. Fox, T. Keith, M. A. Al-Laham, C. Y. Peng, A. Nanayakkara, M. Challacombe, P. M. W. Gill, B. Johnson, W. Chen, M. W. Wong, C. Gonzalez, and J. A. Pople, Gaussian, Inc., Wallingford CT, 2004.